EUROPHYSICS LETTERS 1 April 2001

Europhys. Lett., **54** (1), pp. 45–50 (2001)

Velocity fluctuations and hydrodynamic diffusion in sedimentation

M.-C. Miguel and R. Pastor-Satorras

The Abdus Salam International Centre for Theoretical Physics (ICTP)
P.O. Box 586, 34100 Trieste, Italy

(received 13 November 2000; accepted 23 January 2001)

PACS. 45.70.Qj – Pattern formation.
PACS. 05.40.-a – Fluctuation phenomena, random processes, noise, and Brownian motion.
PACS. 82.70.Kj – Emulsions and suspensions.

Abstract. – We study non-equilibrium velocity fluctuations in a model for the sedimentation of non-Brownian particles experiencing long-range hydrodynamic interactions. The complex behavior of these fluctuations, the outcome of the collective dynamics of the particles, exhibits many of the features observed in sedimentation experiments. In addition, our model predicts a final relaxation to an anisotropic (hydrodynamic) diffusive state that could be observed in experiments performed over longer time ranges.

Despite the fact that the study of sedimenting suspensions has a long and well-deserved history for their ubiquitous nature and applications [1], attention to the non-equilibrium density and velocity fluctuations in these systems has only been paid lately. In particular, the nature of non-equilibrium fluctuations in the sedimentation process has been a subject of a long controversy. While theoretical arguments [2] and extensive computer simulations [3] suggested that velocity fluctuations should diverge with the system size, the available experimental results [4, 5], and the theoretical analysis in ref. [6], found no evidence for such divergences. These apparently contradictory observations may have found a reasonable interpretation after the experimental evidence in ref. [7], and the theoretical study by Levine *et al.* [8].

Another striking piece in the puzzle of sedimentation was recently added by the experimental work of Rouyer *et al.* [9]. In their experiment, the authors analyzed the trajectories and velocities of non-Brownian [10] particles sedimenting in a quasi–two-dimensional (2d) fluidized bed, and showed the intrinsic non-Gaussian nature of velocity fluctuations. The main conclusions of this work are the non-Gaussian form of the probability density functions (PDFs) of the velocity fluctuations; the anisotropic character of the particle trajectories (diffusive along the horizontal direction and superdiffusive along the vertical one); and the presence of very long-range correlations in the velocity fluctuations along the gravity direction. New evidence along some of these lines is also provided in a recent paper by Cowan *et al.* [11].

The results of refs. [7, 9, 11] pose new questions regarding the process of sedimentation, which have not been addressed by previous theoretical approaches. Our purpose in this letter is to tackle these questions from the point of view of the particle's dynamics to ascertain the chief physical mechanisms underlying such fluctuation phenomena. In order to do so, we propose a model of sedimentation in which particles experience long-range hydrodynamic interactions. We start from the solution of the linear Navier-Stokes equation for the suspension in an unbounded incompressible fluid [1]. We consider a system of N particles obeying a system

of coupled differential equations which we solve numerically. In the solution of the equations, we keep track of both positions and velocities of the particles, and compute several relevant statistical properties. In our model, we observe most of the experimental features reported in refs. [7, 9, 11], namely, slow and fast particles, and swirls and channels in the velocity field, which, overall, yield non-Gaussian velocity distributions and a slow time relaxation of the velocity autocorrelations. In addition, our model predicts a final relaxation to an anisotropic (hydrodynamic) diffusive state, not observed in ref. [9].

The velocity of a particle n in a dilute suspension is given by the expression $\boldsymbol{U}_n = \sum_m \boldsymbol{H}_{nm} \cdot \boldsymbol{F}_m$, where the sum is carried out over all the particles m in the suspension, $\boldsymbol{H}_{nm}$ is the mobility tensor, and $\boldsymbol{F}_m$, the external force acting on each particle, is gravity $\boldsymbol{g}$, oriented along the positive z-axis [1]. The simplest form of the tensor $\boldsymbol{H}$ corresponds to dilute suspensions of point-like particles. In this case, the solution of the stationary Navier-Stokes equation in an unbounded medium yields the so-called Oseen tensor $\boldsymbol{H}_0(\boldsymbol{r}) = (\boldsymbol{I} + \boldsymbol{r} \otimes \boldsymbol{r}/r^2)/8\pi\eta r$ [12], where $\boldsymbol{I}$ is the identity matrix, the operator $\otimes$ stands for the tensorial product, and η is the fluid viscosity.

We study a suspension of monodisperse non-Brownian particles (for which inertial effects are irrelevant in a viscous fluid) at very low concentrations, where the point-particle assumption is indeed a good approximation. Initially, particles are placed on the same vertical xz plane. The form of the mobility matrix in the Oseen approximation ensures that particles in such a configuration will never leave that plane. Simulations are performed on a system of N particles in a square cell of size L (corresponding to a concentration $c = N/L^2$). Periodic boundary conditions (PBCs) are imposed in all directions (including the y-direction perpendicular to the initial plane) in order to guarantee the uniformity of the suspension [13]. To avoid the discontinuities arising from truncating long-range hydrodynamic interactions, imposing PBCs amounts to considering Oseen interactions with an infinite set of images of the original system [14]. In this way, the velocity of each particle is written as $\boldsymbol{U}_n = \sum_m \sum_{\boldsymbol{d}} \boldsymbol{H}_0(\boldsymbol{r}_{nm} + \boldsymbol{d}) \cdot \boldsymbol{g}$, where the index m runs through all the particles inside a cell of volume V, $\boldsymbol{r}_{nm}$ indicates the relative position of a pair of particles within that cell, and $\boldsymbol{d}$ runs through the positions of the images of m in an infinite number of cell replicas along the x, y, and z axes.

Imposing PBCs along the y-axis is mathematically equivalent to imposing slip boundary conditions to the fluid velocity field on effective walls parallel to the sedimentation plane, and located at distances $\pm L_y/2$, where $L_y < L$. Sedimentation experiments are usually carried out within a thin fluid slab confined by parallel glass plates. A realistic modelization of this process should thus include wall effects by imposing no-slip boundary conditions on the walls. By doing so, hydrodynamic interactions become exponentially screened for length scales larger than the slab thickness L_y. One then expects that exponentially damped interactions introduce an external characteristic length into the problem, L_y, which will govern the dynamics of the system, a fact that has not been pointed out in the experiments. On the other hand, short-range interactions severely restrict the extent of the correlations, and render the dynamics essentially diffusive on all length scales, preventing the system from showing the collective behavior reported in the experiments. We have checked this last point by performing simulations of a system with real walls at distances comparable to the average interparticle separation. In particular, with our initial conditions one obtains a sum of modified Bessel functions which decay exponentially fast for length scales greater than L_y. As expected, after a short ballistic transient, we observe an essentially diffusive behavior, quite different indeed from the data reported in refs. [7, 9, 11]. We thus conclude that long range interactions must be preserved in order to account for the scale competition observed in the system. Our model is based on this simple consideration.

To compute $\boldsymbol{U}_n$, we resort to the Ewald summation method [14], which yields the following expression:

$$\begin{aligned}\boldsymbol{M}(\boldsymbol{r}) \;&\equiv\; \sum_{\boldsymbol{d}} \boldsymbol{H}_0(\boldsymbol{r}+\boldsymbol{d}) = \\ &= \frac{1}{8\pi\eta}\sum_{\boldsymbol{d}}\left\{\frac{\operatorname{erfc}\left(\frac{|\boldsymbol{r}+\boldsymbol{d}|}{2\beta}\right)}{|\boldsymbol{r}+\boldsymbol{d}|}\,\boldsymbol{I} + \left[\frac{\operatorname{erfc}\left(\frac{|\boldsymbol{r}+\boldsymbol{d}|}{2\beta}\right)}{|\boldsymbol{r}+\boldsymbol{d}|} + \frac{e^{-\left(\frac{|\boldsymbol{r}+\boldsymbol{d}|}{2\beta}\right)^2}}{\sqrt{\pi}\beta}\right]\frac{(\boldsymbol{r}+\boldsymbol{d})\otimes(\boldsymbol{r}+\boldsymbol{d})}{|\boldsymbol{r}+\boldsymbol{d}|^2}\right\} + \\ &+ \frac{1}{\eta V}\sum_{\boldsymbol{G}}\frac{e^{i\boldsymbol{G}\cdot\boldsymbol{r}}\; e^{-\beta^2 G^2}}{G^2}\left[\boldsymbol{I} - (1+\beta^2G^2)\frac{\boldsymbol{G}\otimes\boldsymbol{G}}{G^2}\right]. \qquad (1)\end{aligned}$$

Here the function $\operatorname{erfc}(x)$ is the complementary error function, and β is a parameter which controls the convergence of both the $\boldsymbol{d}$ and $\boldsymbol{G}$ sums. The reciprocal space vectors $\boldsymbol{G}$ are such that $\boldsymbol{G}\cdot\boldsymbol{d} = 2\pi k$, where k is an integer. The terms proportional to $\boldsymbol{I}$ are the same as for the Coulomb potential [14]; the other terms are intrinsic to the Oseen tensor. As in the Coulomb case, the term $\boldsymbol{G} = 0$ in eq. (1) yields a divergent contribution. In the electrostatic case, this infinite contribution cancels out after imposing an overall *charge neutrality* condition. In the sedimentation problem, the $\boldsymbol{G} = 0$ term cancels out after subtracting the mean sedimentation velocity $\boldsymbol{U}^M = (N/V)\int \mathrm{d}^3\boldsymbol{r}\boldsymbol{H}_0(\boldsymbol{r})\cdot\boldsymbol{g}$, and thus working with velocity fluctuations $\boldsymbol{u}_n = \boldsymbol{U}_n - \boldsymbol{U}^M$. By doing so, the particle positions are on average fixed, as in the sedimentation experiments in a fluidized bed.

To follow the evolution of the trajectories and velocities of N particles, we integrate numerically the $2N$ coupled equations $\mathrm{d}\boldsymbol{r}_n/\mathrm{d}t = \sum_m \boldsymbol{M}(\boldsymbol{r}_n - \boldsymbol{r}_m)\cdot\boldsymbol{g} - \boldsymbol{U}^M$, where $\boldsymbol{M}$ is given by eq. (1), using an adaptive step-size fifth-order Runge-Kutta algorithm [15]. We have chosen a convergence parameter $\beta = L/12$; other values of β were also tested, yielding equivalent results. Simulations start from a configuration of N particles randomly placed on a square cell of size L. Since the Oseen approximation is not valid at short distances, to avoid singularities in the velocity field we have introduced an *ad hoc* very short-range repulsive hard-core term of the form $\exp[-(r-2a)/\rho]$, where a is the radius of the particles and ρ is a small parameter that we select equal to 0.1.

The concentrations described by our model are severely limited by both the range of validity of the Oseen approximation and the available CPU time. In our simulations, therefore, we have considered concentrations $c \leq 1\%$, and cell sizes ranging from $L = 100a$ to $L = 200a$. We shall see, however, that our results for dilute concentrations already exhibit most of the salient features reported in the literature. Averages were made over at least 100 realizations starting with different random initial conditions.

In the evolution of our model, particles build up a complex and highly fluctuating pattern of velocity swirls and channels, very similar to those experimentally observed [7,9]. In fig. 1a), we show a snapshot of a system with concentration $c = 1\%$ and cell size $L = 200a$. The number of swirls and their sense of flow (clock- or anticlock-wise) result from the collective interactions, and have the constraint of zero global vorticity $\sum_n \nabla\times\boldsymbol{u}_n = 0$, as follows from the symmetries of the Oseen tensor.

At large times, the average root-mean-square velocity fluctuations (RMSVF) along the horizontal, $\bar{u}_x$, and vertical, $\bar{u}_z$, directions grow with the concentration c. As naively expected from the symmetry breaking induced by gravity, fluctuations are anisotropic. We measure a ratio $\bar{u}_z/\bar{u}_x \simeq 2.5$, which seems independent of c or L. This observation agrees with the results reported in ref. [7].

Next, we have measured the probability density function (PDF) of the velocity fluctuations, $p(u_z)$ and $p(u_x)$, normalized so as to have zero mean and unity standard deviation. In fig. 2 we

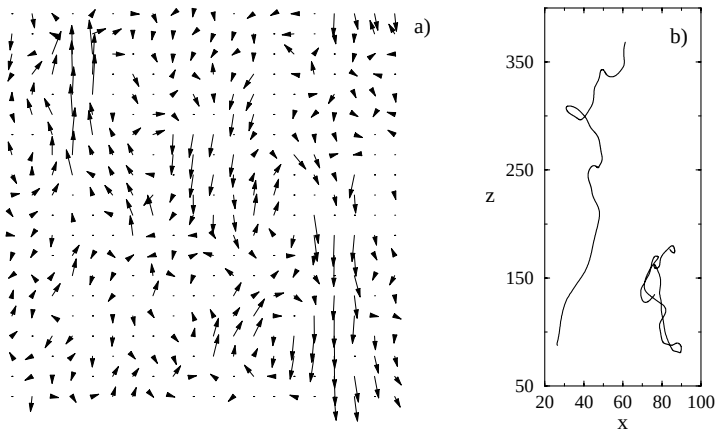

Fig. 1 – a) Snapshot of the velocity fluctuations, showing both swirls and channels. b) Trajectories of a fast (left) and a slow (right) particles (see text). Units given in particle radii.

plot the integrated distribution functions $P_+(u) = \int_u^\infty p(u')\mathrm{d}u'$ for the downward (rightward), $u > 0$, velocity, and $P_-(-u) = \int_{-\infty}^u p(u')\mathrm{d}u'$ for the upward (leftward), $u < 0$, velocity, for both vertical and horizontal fluctuations. In particular, the plots correspond to values of $c = 1\%$ and $L = 200a$. We observe that the horizontal fluctuations are left-right symmetric and very well approximated by a Gaussian distribution (solid line in fig. 2a)). On the other hand, vertical fluctuations are fairly asymmetric and apparently non-Gaussian.

We now turn our attention to the two-time statistical properties of the velocity fluctuations. First, we consider the velocity autocorrelation function $g_\alpha(t) = \langle u_\alpha(0)u_\alpha(t)\rangle \,/\, \langle u_\alpha(0)^2\rangle$, for $\alpha = x, z$, where the brackets denote an average over particles and realizations, at a fixed time t. In fig. 3 we depict $g_\alpha(t)$ for two different concentrations, $c = 1\%$ (system I), represented with ($\circ$), and $c = 0.25\%$ (system II), represented with ($\times$), in a box of size $L = 200$, as well as $c = 1\%$ in a smaller box of size $L = 100$ (system III) which we plot with ($\triangle$). The main plot represents our data as a function of the rescaled time ct; raw data are shown in the inset. For both g_x and g_z, we observe an initial exponential decay of the correlations with a characteristic time proportional to c^{-1}. This scaling of g_α at short times can be understood by means of a simple mean-field–like argument: Given the expression of the Oseen tensor, the velocity correlations can be written as $\langle u(t)u(0)\rangle \sim \langle u(0)/r(t)\rangle$, where r is the separation between any pair of

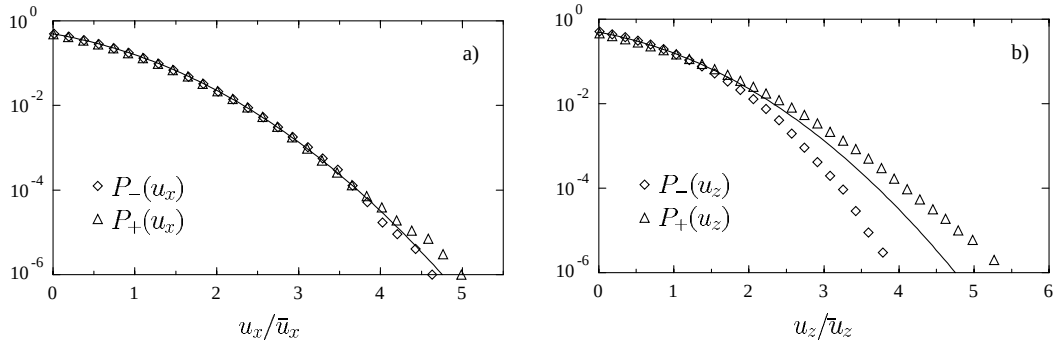

Fig. 2 – Integrated distributions P_+ and P_- for the (a) u_x and (b) u_z velocity fluctuations in linear-log scale. The solid line corresponds to an integrated Gaussian distribution.

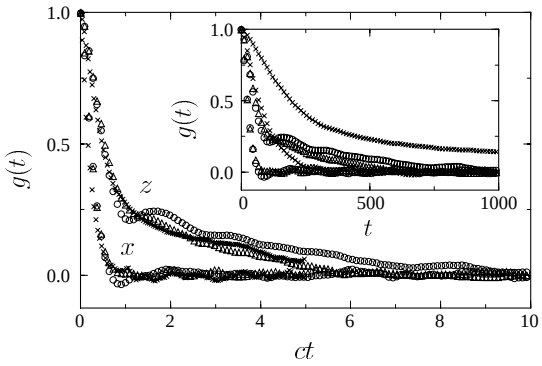

Fig. 3

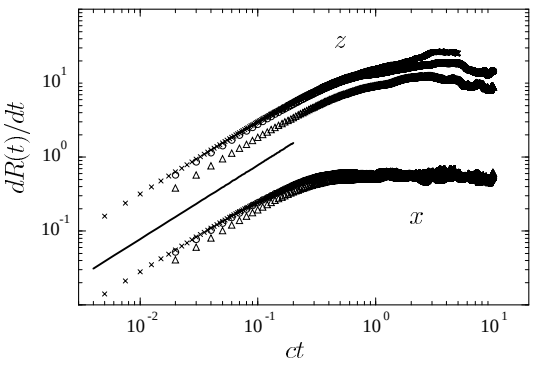

Fig. 4

Fig. 3 – Velocity autocorrelations as a function of time. The curves shown in the inset correspond to the raw data, whereas in the main plot time has been rescaled by the characteristic time $\tau \sim c^{-1}$. ∘ System I, × system II, △ system III (see text).

Fig. 4 – Time derivative of the mean-square displacement in a double logarithmic scale. The solid line with slope 1 represents the ballistic regime.

particles. Taking a time derivative, $\partial_t \langle u(t)u(0)\rangle \sim \partial_t \langle u(0)/r(t)\rangle \sim -\langle u(t)u(0)/r^2\rangle$, where in the second step we have commuted derivative and average. A further simplification considers $r \sim c^{-1/2}$, *i.e.*, the average separation between particles. Then, we have $\partial_t \langle u(t)u(0)\rangle \sim -\langle u(t)u(0)\rangle / c^{-1}$, yielding an exponential relaxation with characteristic time $\tau \sim c^{-1}$.

After this initial decay, the x correlations of the more concentrated system I show a clear negative region. Curiously, this behavior resembles that of a dense liquid. Negative autocorrelations in a dense liquid are due to backscattering effects after collisions among molecules. In our system, however, negative correlations are due to the permanence of the particles in a velocity swirl. As argued in [9], during the course of a simulation some of the particles become part of velocity swirls and spend in them a considerable amount of time. They can be called *slow* particles and describe coil-like trajectories. Others (*fast* particles) spend more time inside the channels separating swirls, and their trajectories are much more elongated. Both channels and swirls can be observed in fig. 1a). In fig. 1b), we plot typical trajectories of a fast and a slow particle.

At later times the correlations of the x components oscillate around zero, whereas the z autocorrelations go through a second regime of much slower relaxation, and eventually become zero towards the end of the simulation time. This enhancement of the z autocorrelations is due to the very existence of channels between swirls, inside of which particles follow ballistic trajectories with small fluctuations. Channels are interrupted by swirls, but since these must be created in pairs of opposite vorticity (due to vorticity conservation), their creation is costly and only a few are present in a box of small size. A long time is thus required for the particles initially in a channel to become part of a few velocity swirls and uncorrelate from their initial conditions.

To further explore the behavior of the system at long times, we have also studied the mean-square displacement of the particles, $R_\alpha(t) = \left\langle [r_\alpha(t) - r_\alpha(0)]^2 \right\rangle$, which is an efficient indicator of a possible effective diffusive behavior of the system (hydrodynamic diffusion) [3]. For the latter, we expect $R_\alpha(t) = 2D_\alpha t$, *i.e.*, $\mathrm{d}R_\alpha(t)/\mathrm{d}t = 2D_\alpha \equiv$ const, where D_α is an effective diffusion coefficient. In fig. 4 we represent the time derivative of $R_\alpha(t)$ for the displacements along the x and z directions. The plateau at long times clearly indicates that

the displacement along the x-direction becomes purely diffusive right after an initial ballistic regime ($R_x(t) \sim t^2$). The z displacement also becomes eventually diffusive, but at longer times scales. This final diffusive behavior is compatible with the fast decay of the tails of the PDFs shown in fig. 2. We observe that $D_z \gg D_x$, hence the diffusive regime is highly anisotropic. At intermediate times, we observe that $R_z(t)$ can be fitted to a power law $R_z(t) \sim t^\alpha$ with an exponent within the range 1-2. Such behavior was reported in [9], where experiments could not be run for long enough times as in our simulations. We expect that experiments carried out over longer time scales would also show the eventual diffusive behavior along the vertical direction.

To sum up, we present a model for the sedimentation of non-Brownian particles in an unbounded fluid that incorporates long-range hydrodynamic interactions and PBCs in the simplest Oseen approximation. This model exhibits most of the salient features of the experiments reported in refs. [7, 9, 11]. Our findings can be understood within the picture of slow and fast particles: Slow particles spend most of the time within velocity swirls and contribute to the fast relaxation of the velocity correlations. Fast particles moving along velocity channels have strongly correlated (quasi-ballistic) trajectories and are responsible for the slow relaxation component. For sufficiently long times, all particles become part of enough velocity swirls, and our model predicts that the system eventually relaxes to a hydrodynamic diffusive regime, that could be confirmed by experiments performed over longer time spans.

* * *

We thank S. Franz, M. Kardar, I. Pagonabarraga, M. Rubí, and A. Vespignani, for helpful discussions. The work of RPS has been supported by the TMR Network ERBFMRXCT980183.

REFERENCES

[1] Russel W., Saville D. and Schowalter W., *Colloidal Dispersions* (Cambridge University Press, Cambridge) 1995.
[2] Caflisch R. and Luke J., *Phys. Fluids*, **28** (1985) 259.
[3] Ladd A., *Phys. Rev. Lett.*, **76** (1996) 1392.
[4] Nicolai H. and Guazzelli E., *Phys. Fluids*, **7** (1995) 3.
[5] Xue J.-Z., Herbolzeimer E., Rutger M. A., Russel W. B. and Chaikin P.M., *Phys. Rev. Lett.*, **69** (1992) 1715.
[6] Koch D. and Shaqfeh E., *J. Fluid Mech.*, **224** (1991) 275.
[7] Segrè P., Herbolzheimer E. and Chaikin P., *Phys. Rev. Lett.*, **79** (1997) 2574.
[8] Levine A., Ramaswamy S., Frey E. and Bruinsma R., *Phys. Rev. Lett.*, **81** (1998) 5944.
[9] Rouyer F., Martin J. and Salin D., *Phys. Rev. Lett.*, **83** (1999) 1058.
[10] Particles for which the diffusive motion caused by the surrounding solvent is negligible.
[11] Cowan M. L., Page J. H. and Weitz D. A., *Phys. Rev. Lett.*, **85** (2000) 453.
[12] Note that the self-interaction term $\sim \boldsymbol{I}/6\pi\eta a$ has been omitted since we are interested in velocity *fluctuations*.
[13] Spurious results emerge from the boundary discontinuity of the density when imposing open boundary conditions.
[14] Rapaport D., *The Art of Molecular Dynamics Simulation* (Cambridge University Press, Cambridge) 1995.
[15] Press W. H., Flannery B. P., Teukolsky S. A. and Vetterling W. T., *Numerical Recipes in C: The Art of Scientific Computing*, 2nd edition (Cambridge University Press, Cambridge) 1992.